

Electronic Supplementary Information

Unravelling the Strain-Promoted [3+2] Cycloaddition Reactions of Phenyl Azide with Cycloalkynes within the Molecular Electron Density Theory Perspective

Luis R Domingo^{1*} and Nivedita Acharjee²

¹ Department of Organic Chemistry, University of Valencia, Dr. Moliner 50, Burjassot, E-46100 Valencia, Spain; Contact: domingo@utopia.uv.es

² Department of Chemistry, Durgapur Government College, J. N. Avenue, Durgapur-, West Bengal 713214, India; Contact: nivchem@gmail.com

Index

- S1** BET study of the 32CA reaction of phenyl azide **3** with cyclohexyne **C6**.
- S5** BET study of the 32CA reaction of phenyl azide **3** with 2-butyne **13**.
- S8** References.
- S9** Figure with the natural atomic charges of the reagents.
- S10** Table with the MPWB1K/6-311G(d,p) calculated CDFT indices at the ground state of the reagents.
- S10** Figure with plot of the MPWB1K/6-311G(d,p) gas phase electrophilicity ω indices vs the B3LYP/6-31G(d) ones of phenyl azide **3**, cycloalkynes **C5 - C9** and 2-butyne **13**.
- S11** Table with the MPWB1K/6-311G(d,p) calculated electronic energies, enthalpies and Gibbs free energies, in kcal·mol⁻¹, computed at 298 K in gas phase of the stationary points involved in the 32CA reactions of phenyl azide **3** with cycloalkyne series **C5 - C9** and 2-butyne **13**.
- S12** Table with the MPWB1K/6-311G(d,p) calculated electronic energies, enthalpies and Gibbs free energies, in kcal·mol⁻¹, computed at 298 K in acetonitrile of the stationary points involved in the 32CA reactions of phenyl azide **3** with cycloalkyne series **C5 - C9** and 2-butyne **13**.

1. BET study of the 32CA reaction of phenyl azide **3** with cyclohexyne **C6**

The Bonding evolution theory¹ (BET) comes from the conjunction of ELF topological analysis^{2,3} and Thom's Catastrophe theory⁴ and has proven to be a very useful methodological tool to establish the nature of the electronic rearrangement associated along the reaction path.⁵ Herein, the BETs of the 32CA reactions of phenyl azide **3** with cyclohexyne **C6** and with 2-butyne **13** are studied.

The 32CA reaction of phenyl azide **3** with **C6** takes place along eight different phases (see Table S1). *Phase I* starts at **S0-I**, $d_{C4-N3} = 2.97 \text{ \AA}$ and $d_{C5-N1} = 2.64 \text{ \AA}$, which corresponds with the first structure of the IRC. ELF of **S0-I** is similar to that of the separated reagents (see section 3.1), except the formation of monosynaptic $V(C4)$ integrating at 1.04 e, which mainly comes from the depopulation of the electron density of C4-C4' single bond adjacent to the alkyne framework. The disynaptic basin $V(C4,C4')$ undergoes depopulation from 2.71 e in **1** to 1.90 e in **S0-I**.

The short phase *Phase II* starts at **S1-I**, $d_{C4-N3} = 2.93 \text{ \AA}$ and $d_{C5-N1} = 2.59 \text{ \AA}$. The two $V(N2,N3)$ and $V'(N2,N3)$ disynaptic basins present at **S0-I** have merged into a new $V(N2,N3)$ disynaptic basin, integrating 4.26 e. The short phase *Phase III* starts at **S2-I**, $d_{C4-N3} = 2.80 \text{ \AA}$ and $d_{C5-N1} = 2.49 \text{ \AA}$. The disynaptic $V(C4,C5)$ disynaptic basins present at **S1-I** has split into a two disynaptic basins $V(C4,C5)$ and $V'(C4,C5)$, respectively integrating at 2.24 e and 2.23 e.

Phase IV starts at **S3-I**, $d_{C4-N3} = 2.71 \text{ \AA}$ and $d_{C5-N1} = 2.43 \text{ \AA}$, which is characterised by the creation of a new $V(N2)$ monosynaptic basin, integrating 0.47 e, associated with the formation of a lone pair at the N2 nitrogen. The electron density of this lone pair mainly comes from the depopulation of the N1-N2 and N2-N3 bonding regions along *Phase III*. In this phase, **TS1** is found. These bonding changes demand an energy cost of 2.2 kcal·mol⁻¹.

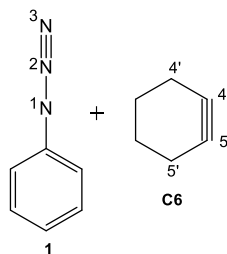
Phase V starts at **S4-I**, $d_{C4-N3} = 2.20 \text{ \AA}$ and $d_{C5-N1} = 1.98 \text{ \AA}$, which is characterised by the creation of a new $V(C5)$ monosynaptic basin, integrating 0.18 e, associated with the formation of a *pseudoradical* center at the C5 carbon. Together with this change, the $V(C4,C5)$ disynaptic basin experiences a depopulation of 0.30 e along *Phase IV*.

Phase VI starts at **S5-I**, $d_{C4-N3} = 2.13 \text{ \AA}$ and $d_{C5-N1} = 1.91 \text{ \AA}$. At the beginning of this phase the first more relevant change along the IRC takes place. At this structure, while the $V(C5)$ monosynaptic basin present at **S4-I** is missing, a new $V(N1,C5)$ disynaptic basin, integrating 1.39 e, is created. This topological changes indicate that the formation of the first

N1-C5 single bond has begun at a C–N distance of 1.91 Å. Together with this change, the monosynaptic V(N1) basin experiences a depopulation of 1.10 e along *Phase V*.

Phase VII starts at **S6-I**, $d_{C4-N3} = 1.95$ Å and $d_{C5-N1} = 1.73$ Å. At this structure, the V(N3) monosynaptic basin present at **S5-I** splits in two V(N3) and V'(N3) monosynaptic basins, integrating 3.34 e and 0.40 e, respectively.

Table S1. ELF valence basin populations, distances of the forming bonds, and relative^a electronic energies of the gas phase IRC structures **S0-I** – **S7-I** defining the eight phases characterizing the molecular mechanism of the 32CA reaction between phenyl azide **3** with cyclohexyne **C6** yielding 1,2,3-triazole **8**. Distances are given in angstroms, Å, and relative energies in kcal·mol⁻¹.



Phases	<i>I</i>	<i>II</i>	<i>III</i>	<i>IV</i>	<i>V</i>	<i>VI</i>	<i>VII</i>	<i>VIII</i>	
Structures	S0-I	S1-I	S2-I	S3-I	S4-I	S5-I	S6-I	S7-I	8
d(C4–N3)	2.968	2.925	2.796	2.713	2.200	2.134	1.951	1.727	1.348
d(C5–N1)	2.635	2.594	2.493	2.431	1.979	1.912	1.727	1.551	1.351
ΔE	0.0	0.3	1.4	2.2	-3.9	-8.9	-29.2	-58.8	-115.0
V(N1)	3.30	3.29	3.27	3.26	3.30	2.20	2.00	1.83	1.18
V'(N2)				0.47	2.24	2.35	2.59	2.79	3.13
V(N1,N2)	2.48	2.47	2.40	2.33	1.75	1.72	1.67	1.65	1.74
V(N2,N3)	1.65	4.26	4.34	3.96	2.87	2.80	2.65	2.48	2.08
V'(N2,N3)	2.59								
V(N3)	3.66	3.65	3.64	3.63	3.64	3.66	3.34	3.10	2.88
V'(N3)							0.40		
V(C4,C5)	4.47	4.47	2.24	2.29	2.07	2.03	1.97	1.89	3.47
V'(C4,C5)			2.23	2.16	2.08	2.05	1.95	1.94	
V(C4,C4')	1.90	1.89	1.88	1.87	1.94	1.96	2.01	2.04	2.08
V(C5,C5')	2.41	2.40	2.39	2.38	2.26	2.19	2.11	2.08	2.11
V(C4)	1.04	1.06	1.10	1.13	1.16	1.15	1.05		
V(C5)					0.18				
V(N3,C4)								1.66	2.28
V(N1,C5)						1.39	1.77	2.03	2.41

Finally, the last *Phase VIII* starts at **S7-I**, $d_{C4-N3} = 1.73 \text{ \AA}$ and $d_{C5-N1} = 1.55 \text{ \AA}$, and ends at 1,2,3-triazole **6**, $d_{C4-N3} = 1.35 \text{ \AA}$ and $d_{C5-N1} = 1.35 \text{ \AA}$. At **S7-I** the second more relevant change along the IRC takes place. At this structure, while the $V(C4)$ and $V'(N3)$ monosynaptic basins are missing, a new $V(N3,C4)$ disynaptic basin, integrating 1.66 e, is created. These relevant topological changes indicate that the formation of the second N3–C4 single bond has begun at a C–N distance of 1.73 \AA , through the C-to-N coupling of the electron density of the C4 *pseudoradical* carbon (integrating 1.05 e) and part of the non-bonding electron density of the N3 nitrogen. Along this last phase, the molecular electron density is relaxed to reach the structure of 1,2,3-triazole **8**, in which the population of the $V(N3,C4)$ and $V(N1,C5)$ disynaptic basins reach a population of 2.28 and 2.41 e, respectively.

2. BET study of the 32CA reaction of phenyl azide **3** with 2-butyne **13**

The 32CA reaction of phenyl azide **3** with 2-butyne **13** takes place along nine different phases (see Table S2). *Phase I* starts at **S0-II**, $d_{C4-N3} = 3.02 \text{ \AA}$ and $d_{C5-N1} = 2.91 \text{ \AA}$, which corresponds with the first structure of the IRC. ELF of **S0-II** is similar to that of the separated reagents (see section 3.1).

The short phase *Phase II* starts at **S1-II**, $d_{C4-N3} = 2.78 \text{ \AA}$ and $d_{C5-N1} = 2.72 \text{ \AA}$. At this structure the two $V(N2,N3)$ and $V'(N2,N3)$ disynaptic basins present at **S0-II** have merged into a $V(N2,N3)$ disynaptic basin, integrating 4.21 e. This phase demands an energy cost of $3.8 \text{ kcal}\cdot\text{mol}^{-1}$.

Phase III starts at **S2-II**, $d_{C4-N3} = 2.53 \text{ \AA}$ and $d_{C5-N1} = 2.55 \text{ \AA}$, which is characterised by the creation of a new $V(N2)$ monosynaptic basin, integrating 0.58 e, associated with the formation of a lone pair at the N2 nitrogen. The electron density of this lone pair mainly comes from the depopulation of the N1–N2 and N2–N3 bonding regions, which experience depopulation of 0.15 e and 0.41 e along *Phase II*. These bonding changes demand an energy cost of $10.9 \text{ kcal}\cdot\text{mol}^{-1}$.

The short phase *Phase IV* starts at **S3-II**, $d_{C4-N3} = 2.32 \text{ \AA}$ and $d_{C5-N1} = 2.41 \text{ \AA}$. At **S3-II** the $V(C4,C5)$ disynaptic basin is split in two new disynaptic basin, $V(C4,C5)$ and $V'(C4,C5)$, integrating 2.79 and 2.62 e, respectively. These bonding changes demand an energy cost of $18.7 \text{ kcal}\cdot\text{mol}^{-1}$.

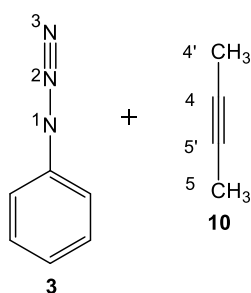
Phase V starts at **S4-II**, $d_{C4-N3} = 2.00 \text{ \AA}$ and $d_{C5-N1} = 2.20 \text{ \AA}$, which is characterised for the creation of a new $V(C4)$ monosynaptic basin, integrating 0.30 e, associated with the formation of a *pseudoradical* center at the C4 carbon. Together with this change, the $V(C4,C5)$ disynaptic basin undergoes a depopulation of 0.45 e along *Phase IV*. These bonding changes demand an energy cost of $24.2 \text{ kcal}\cdot\text{mol}^{-1}$.

Phase VI starts at **S5-II**, $d_{C4-N3} = 1.82 \text{ \AA}$ and $d_{C5-N1} = 2.08 \text{ \AA}$. At this structure, the $V(N3)$ monosynaptic basin presents at **S4-II** is split in two $V(N3)$ and $V'(N3)$ monosynaptic basins, integrating 3.46 and 0.39 e, respectively.

Phase VII starts at **S6-II**, $d_{C4-N3} = 1.74 \text{ \AA}$ and $d_{C5-N1} = 2.02 \text{ \AA}$, which is characterised for the creation of a new $V(C5)$ monosynaptic basin, integrating 0.13 e, associated with the formation of a *pseudoradical* center at the C5 carbon. Together with this change, the $V(C4,C5)$ disynaptic basin undergoes a depopulation of 0.22 e along *Phase VI*. These bonding changes demand an energy cost of $12.4 \text{ kcal}\cdot\text{mol}^{-1}$.

Phase VIII starts at **S7-II**, $d_{C4-N3} = 1.70 \text{ \AA}$ and $d_{C5-N1} = 1.99 \text{ \AA}$. At the beginning of this phase the first more relevant change along the IRC takes place. At this structure, while the $V(C4)$ and $V'(N3)$ monosynaptic basins are missing, a new $V(N3,C4)$ disynaptic basin, integrating 1.33 e, is created. These topological changes indicate that the formation of the first N3–C4 single bond has begun at a C–C distance of 1.70 \AA , through the C-to-N coupling of the two C4 and N3 *pseudoradicals*.

Table S2. ELF valence basin populations, distances of the forming bonds, and relative^a electronic energies of the gas phase IRC structures **S0-I** – **S8-I** defining the nine phases characterizing the molecular mechanism of the 32CA reaction between phenyl azide **3** with 2-butyne **13** yielding 1,2,3-triazole **14**. Distances are given in angstroms, Å , and relative energies in $\text{kcal}\cdot\text{mol}^{-1}$.



Phases	I	II	III	IV	V	VI	VII	VIII	IX	
Structures	S0-II	S1-II	S2-II	S3-II	S4-II	S5-II	S6-II	S7-II	S8-II	14
$d(C4-N3)$	3.017	2.780	2.534	2.317	2.002	1.823	1.743	1.697	1.623	1.350
$d(C5-N1)$	2.909	2.724	2.545	2.405	2.203	2.081	2.023	1.986	1.922	1.354
ΔE	0.0	3.8	10.9	18.7	24.2	18.1	12.4	8.2	0.1	-71.2
$V(N1)$	3.30	3.27	3.25	3.27	3.31	3.32	3.31	3.31	1.98	1.16
$V'(N2)$			0.58	1.54	2.21	2.44	2.53	2.57	2.64	3.13
$V(N1,N2)$	2.52	2.49	2.34	2.09	1.81	1.78	1.79	1.78	1.79	1.75
$V(N2,N3)$	1.70	4.21	3.80	3.12	2.77	2.60	2.54	2.50	2.44	2.07
$V'(N2,N3)$	2.47									
$V(N3)$	3.72	3.71	3.69	3.67	3.75	3.46	3.32	3.27	3.19	2.88
$V'(N3)$						0.39	0.59			
$V(C4,C5)$	1.70	5.21	5.48	2.79	2.46	2.29	2.24	2.20	2.12	3.51
$V'(C4,C5)$	1.82	0.30		2.62	2.50	2.38	2.21	2.17	2.13	--
$V''(C4,C5)$	1.91									
$V'''(C4,C5)$	0.10									
$V(C4,C4')$	2.16	2.17	2.18	2.20	2.24	2.20	2.16	2.15	2.13	2.06
$V(C5,C5')$	2.15	2.16	2.17	2.18	2.13	2.07	2.06	2.06	2.05	2.08
$V(C4)$					0.30	0.55	0.62			
$V(C5)$							0.13	0.16		
$V(C4,N3)$								1.33	1.51	2.28
$V(C5,N1)$									1.54	2.41

Finally, the last *Phase IX* starts at **S8-II**, $d_{C4-N3} = 1.62 \text{ \AA}$ and $d_{C5-N1} = 1.92 \text{ \AA}$, and ends at 1,2,3-triazole **14**, $d_{C4-N3} = 1.35 \text{ \AA}$ and $d_{C5-N1} = 1.35 \text{ \AA}$. At **S8-II** the second more relevant change along the IRC takes place. At this structure, while the V(C5) monosynaptic basin is missing, a new V(N1,C5) disynaptic basin, integrating 1.54 e, is created. These relevant topological changes indicate that the formation of the second C5–N1 single bond has begun, through the C-to-N coupling of the electron density of the C5 *pseudoradical* carbon (integrating 0.16 e) and part of the non-bonding electron density of the N1 nitrogen. Along this last phase, the molecular electron density is relaxed to reach the structure of 1,2,3-triazole **14**, in which the population of the V(N3,C4) and V(N1,C5) disynaptic basins reach a population of 2.28 and 2.41 e, respectively.

References

1. X. Krokidis, S. Noury and B. Silvi, *J. Phys. Chem. A*, 1997, **101**, 7277-7282.
2. A. D. Becke and K. E. Edgecombe, *J. Chem. Phys.*, 1990, **92**, 5397-5403.
3. B. Silvi and A. Savin, *Nature*, 1994, **371**, 683- 686.
4. (a) Thom, R. *Stabilité Structurelle et Morphogénèse*; Interditions, Paris, 1972; (b) A. E. R. Woodcock, T. A. Poston in *Geometrical Study of Elementary Catastrophes*, Spinger-Verlag, Berlin, 1974.
5. (a) V. Polo, J. Andrés, S. Berski, L. R. Domingo and B. Silvi, *J. Phys. Chem. A*. 2008, **112** 7128-7136; (b) J. Andrés, P. González-Navarrete and V. Safont, *Int. J. Quantum Chem.* 2014, **114**, 1239-1252; (c) J. Andrés, S. Berski, L.R. Domingo, V. Polo and B. Silvi. *Curr. Org. Chem.* 2011, **15**, 3566-3575.

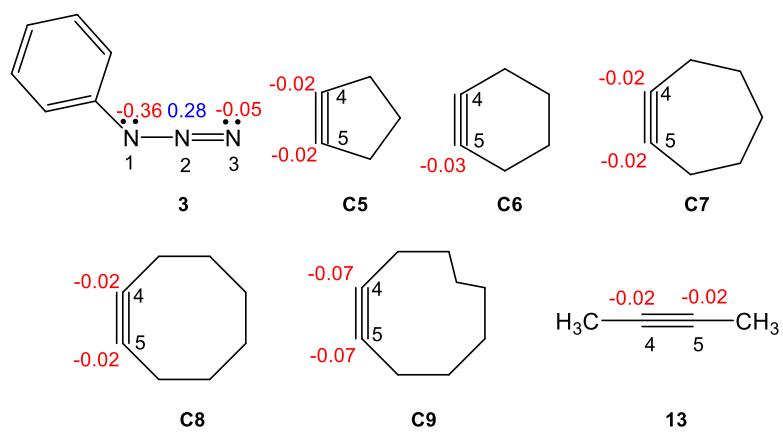


Figure S1. MPWB1K/6-311G(d) calculated gas phase natural atomic charges, in average number of electrons e , of phenyl azide **3**, cycloalkynes series **C5 - C9** and 2-butyne **13**. Negative charges are coloured in red, and positive charges in blue.

Table S3. MPWB1K/6-311G(d,p) calculated gas phase electronic chemical potential μ , chemical hardness η , global electrophilicity ω and global nucleophilicity N , in eV, of phenyl azide **3**, cycloalkyne series **C5 - C9** and 2-butyne **13**.

	μ	η	ω	N
3	-3.62	7.18	0.91	3.18
C5	-4.66	6.11	1.78	2.68
C6	-3.82	7.59	0.96	2.78
C7	-3.27	8.65	0.62	2.80
C8	-2.94	9.63	0.45	2.64
C9	-2.91	9.80	0.43	2.58
13	-2.78	10.23	0.38	2.50

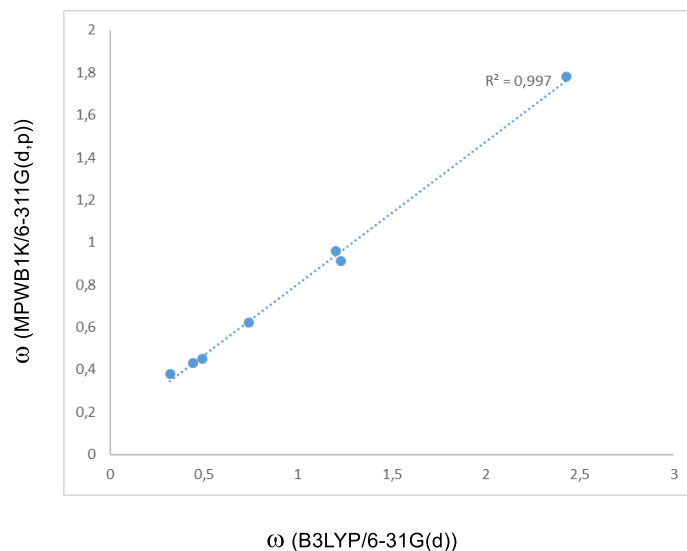


Figure S2. Plot of the MPWB1K/6-311G(d,p) gas phase electrophilicity ω indices vs the B3LYP/6-31G(d) ones of phenyl azide **3**, cycloalkyne series **C5 - C9** and 2-butyne **13**.

Table S4. MPWB1K/6-311G(d,p) calculated electronic energies, E in a.u., enthalpies, H in a.u., and Gibbs free energies, G in a.u., computed at 298 K in gas phase, of the stationary points involved in the 32CA reactions of phenyl azide **3** with cycloalkyne series **C5** - **C9** and 2-butyne **13**.

	E	H	G
3	-395.726968	-395.612629	-395.652220
C5	-193.895898	-193.797192	193.829793
C6	-233.253251	-233.122345	-233.157246
C7	-272.580026	-272.417963	-272.455134
C8	-311.894748	-311.701556	-311.741219
C9	-351.201515	-350.977942	-351.019508
13	-155.919626	-155.826896	-155.863417
TS1	-589.631925	-589.417555	-589.473779
8	-589.843793	-589.622840	-589.671029
TS2	-628.974200	-628.728121	-628.783426
9	-629.163459	-628.911488	-628.961484
TS3	-668.292664	-668.016731	-668.071962
10	-668.460498	-668.178074	-668.230810
TS4	-707.598896	-707.291223	-707.351616
11	-707.751148	-707.437731	-707.492988
TS5	-746.900217	-746.562602	-746.621276
12	-747.047856	-746.704090	-746.761249
TS6	-551.607718	-551.400112	-551.452673
14	-551.760068	-551.546929	-551.596012

Table S5. MPWB1K/6-311G(d,p) calculated electronic energies, E in a.u., enthalpies, H in a.u., and Gibbs free energies, G in a.u., computed at 298 K in acetonitrile, of the stationary points involved in the 32CA reactions of phenyl azide **3** with cycloalkyne series **C5** - **C9** and 2-butyne **13**.

	E	H	G
3	-395.735105	-395.621680	-395.661304
C5	-193.899214	-193.800683	-193.833386
C6	-233.258460	-233.128128	-233.163170
C7	-272.584897	-272.423436	-272.460637
C8	-311.899348	-311.706804	-311.746457
C9	-351.205865	-350.982974	-351.024528
13	-155.922991	-155.831421	-155.863661
TS1	-589.643586	-589.429140	-589.485085
8	-589.854209	-589.633309	-589.681491
TS2	-628.984832	-628.739937	-628.794909
9	-629.179176	-628.928436	-628.978679
TS3	-668.303597	-668.027900	-668.084768
10	-668.476697	-668.195283	-668.247856
TS4	-707.608430	-707.302116	-707.362018
11	-707.767717	-707.455634	-707.511066
TS5	-746.910277	-746.572932	-746.633552
12	-747.063787	-746.721110	-746.778426
TS6	-551.616071	-551.409372	-551.461748
14	-551.775026	-551.563334	-551.613718